Journal of Organometallic Chemistry, 474 (1994) 199–206

Coordination chemistry of $[CH(PPh_2)(P(S)Ph_2)_2]$: Pd, Pt, Rh, and Ir complexes, including the crystal and molecular structures of the ligand and a tripodal iridium complex, $[Ir(cod)\{CH(PPh_2)(P(S)Ph_2)_2\text{-}P,S,S\}]BF_4 \cdot CH_2Cl_2$

Jane Browning, Keith R. Dixon and Sherrie Fang Wang

Department of Chemistry, University of Victoria, P.O. Box 3055, Victoria, B.C., V8W 3P6 (Canada)

(Received October 8, 1993)

Abstract

The complex cations, $[M(cod)\{CH(PPh_2)(P(S)Ph_2)_2\text{-}P,S,S\}]^+$, M = Ir or Rh, and $[MCl(PEt_3)\{CH(PPh_2)(P(S)Ph_2)_2\text{-}P,S\}]^+$, M = Pt or Pd, are readily prepared as fluoroborate salts by reactions of the ligand, $CH(PPh_2)(P(S)Ph_2)_2$, with the chlorobridged complexes, $[M_2Cl_2(cod)_2]$, M = Ir or Rh, cod = cycloocta-1,5-diene, and $[M_2Cl_4(PEt_3)_2]$, M = Pt or Pd, under mild conditions in the presence of $NaBF_4$. Structures are assigned on the basis of ^{31}P NMR spectra and, in the case of M = Ir, by X-ray diffraction. The iridium and rhodium complexes contain tripodal η^3-*P,S,S* coordinated ligands in contrast to the examples for palladium and platinum, where the ligands are bidentate η^2-*P,S* coordinated with the second P=S group non-coordinated ("dangling"). In solution at 25°C, the palladium complex exhibits fluxional behaviour with rapid exchange between the coordinated and "dangling" P=S groups. Both platinum and palladium complexes consist mainly of the isomers having the coordinated P=S group *trans* to Cl, but small quantities of the other isomer are formed for both metals. The ligand **1**, $CH(PPh_2)(P(S)Ph_2)_2$ crystallizes in the $P2_1/n$ (No. 14) space group ($Z = 4$) with $a = 19.867(9)$ Å, $b = 18.889(7)$ Å, $c = 8.828(4)$ Å, $\beta = 100.47(5)°$ and complex **3a**, $[Ir(cod)\{CH(PPh_2)(P(S)Ph_2)_2\text{-}P,S,S\}]BF_4\ CH_2Cl_2$, in the $P\bar{1}$ (No. 2) space group ($Z = 2$) with $a = 10.899(6)$ Å, $b = 21.653(9)$ Å, $c = 11.124(5)$ Å, $\alpha = 85.14(4)°$, $\beta = 111.59(4)°$, $\gamma = 107.93(6)°$. In **3a**, iridium is five-coordinate with an η^3-*P,S,S* ligand and the two double bonds of the cod ligand in an irregular geometry. The structural parameters of the ligand, **1**, are changed relatively little by coordination except for a narrowing of the P–C–P angles.

Key words: Palladium; Platinum; Rhodium; Iridium; Phosphorus; Sulfur

1. Introduction

The phosphine chalcogenides, $CH(P(X)Ph_2)(P(Y)Ph_2)(P(Z)Ph_2)$: X, Y, Z = electron pair or O, S, or Se; have attracted recent attention for several reasons [1–8]. The analogy to the tris(pyrazolyl)borates [9,10], and the general rarity of tripodal anionic ligands prompted study of the derived anions, especially $[C(P(S)Ph_2)_3]^-$. X-ray studies confirmed tripodal η^3-*S,S,S* coordination in the d^{10} complexes, $[HgCl\{C(P(S)Me_2)(P(S)Ph_2)_2\text{-}S,S,S\}]$ [3] and $[Ag(PBu_3)\{C(P(S)Ph_2)_3\text{-}S,S,S\}$ [5]. In complexes with d^8 metals, bidentate η^2-*S,S* coordination proved to be the norm; as demonstrated by structures of $[PtCl(PEt_3)\{C(P(S)Ph_2)_3\text{-}S,S\}]$ [7], $[Rh(cod)\{C(P(S)Ph_2)_3\text{-}S,S\}]$ [8], and $[Ir(CO)_2\{C(P(S)Ph_2)_3\text{-}S,S\}]$ [8]. However, the bidentate complexes are frequently fluxional. The dynamic processes involve rapid exchange between the non-coordinated P=S group and one or both of the coordinated P=S groups, and are suggestive of η^3 intermediates [7,8]. Most recently, phosphine chalcogenide ligands have been shown to promote catalytic activity at some metal centres (especially iridium complexes of $[C(P(O)Ph_2)_3]$) [11–13], and the ready interconversion of η^2 with η^3 coordination is considered important in this activity [13]. However, tripodal coordination has not been structurally confirmed for any complex of this ligand family with a platinum group metal.

We have recently begun study of complexes of $CH(PPh_2)(P(S)Ph_2)_2$ (Scheme 1, structure **1**), and its

---

Correspondence to: Dr. K.R. Dixon.

0022-328X/94/$7.00
SSDI 0022-328X(93)24295-G

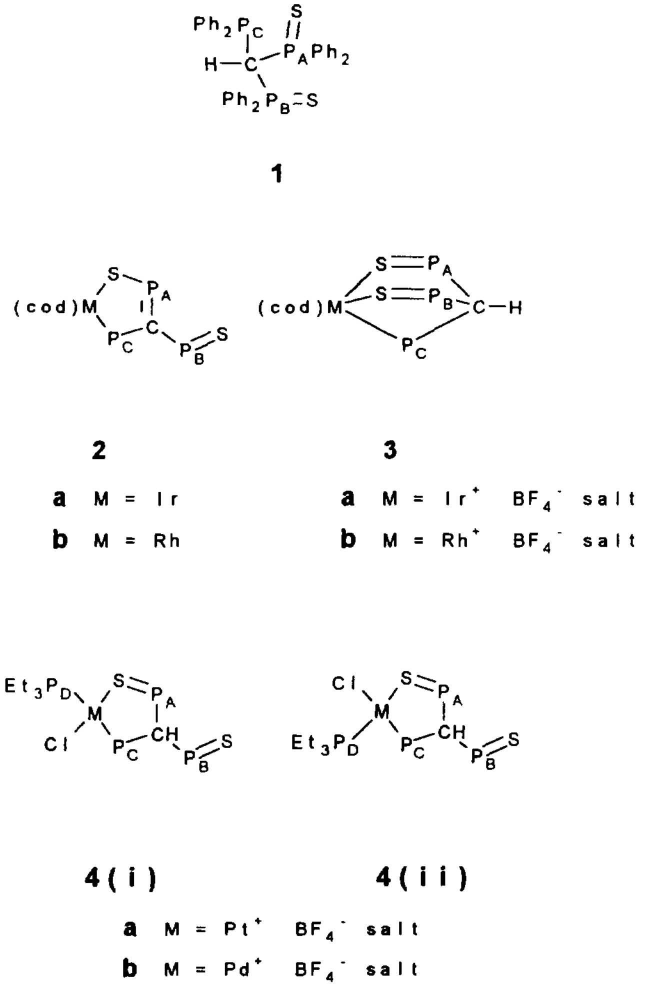

Scheme 1. Structures and atom labelling schemes for compounds 1–4. With the exception of structure 1, the two phenyl groups attached to each phosphorus have been omitted for clarity.

derived anion, [C(PPh$_2$(P(S)Ph$_2$)$_2$], partly to study dynamic processes when one end of the ligand is anchored by a strong M–P bond, but also to search for possible tripodal coordination [14]. In a previous paper we showed that complexes of the anion with d^8 metals (Pt, Rh, and Ir) are bidentate and non-fluxional by ^{31}P NMR, and confirmed η^2-*P,S* coordination by X-ray study of [Rh(cod){C(PPh$_2$)(P(S)Ph$_2$)$_2$-*P,S*}] **2b** [14]. We now report studies of the protonated ligand CH(PPh$_2$)(P(S)Ph$_2$)$_2$. The preferred mode in d^8 metal complexes is tripodal *P,S,S* coordination, and the structure of [Ir(cod){CH(PPh$_2$)(P(S)Ph$_2$)$_2$-*P,S,S*}]BF$_4$ is the first X-ray confirmation of tripodal coordination for a d^8 metal for any member of this triphosphine chalcogenide ligand family, and is thus important in the context of catalytic activity [13]. To our knowledge it is also the first structure on a protonated rather than an anionic ligand of this family. Evidently, the sp^3 geometry of the central carbon in the protonated ligand can accommodate tripodal coordination more easily than the planar sp^2 geometry of the anions.

2. Experimental details

2.1. Synthesis and spectroscopic studies

Data relating to the characterization of the complexes are given in Tables 1–6, in Section 3, and in the preparative descriptions below. Microanalysis was by the Canadian Microanalytical Service, Vancouver, B.C., Canada. Infrared spectra were recorded in KBr disks from 4000 cm^{-1} to 200 cm^{-1} with accuracy ± 3 cm^{-1} on a Perkin-Elmer 1320 grating spectrophotometer calibrated against polystyrene film.

TABLE 1. ^{31}P NMR parameters for CH(PPh$_2$)(P(S)Ph$_2$)$_2$ (LH), and its complexes

Compound		Notes	δ(P$_A$)	δ(P$_B$)	δ(P$_C$)	J(P$_A$–P$_B$)	J(P$_A$–P$_C$)	J(P$_B$–P$_C$)	J(M–P$_A$)	J(M–P$_B$)	J(M–P$_C$)
1	LH	a	—43.5—		−10.0	na	—49—				
3a	Ir(cod)LH$^+$	cd	—52.8—		37.3	na	—39—				
2a	Ir(cod)L	de	65.6	41.7	36.3	47	112	15			
3b	Rh(cod)LH$^+$	bc	—51.4—		46.7	na	—37—		—nr—		134
2b	Rh(cod)L	de	56.0	42.3	39.5	46	115	20	nr	11	134
4a(i)	PtCl(PEt$_3$)LH$^+$	dfg	68.8	35.1	40.8	nr	70	nr	117	nr [h]	2350
	PtCl(PEt$_3$)L	defi	62.8	43.2	34.6	43	110	nr	78	197	2200
4b(i)	PdCl(PEt$_3$)LH$^+$	fj	—52.8—		42.5	na	—39—				

Isomer structures and atom labels are shown in Scheme 1. Chemical shifts (δ) are quoted in parts per million relative to 85% H$_3$PO$_4$. Coupling constants (*J*) are in Hz. nr = not resolved.

[a] CDCl$_3$ solution. Data from ref. 4. [b] Tetrahydrofuran solution. [c] The P$_A$ and P$_B$ resonances are equivalent (see text). [d] Dichloromethane solution with an external C$_6$D$_6$ lock. [e] Data from ref. 14. [f] Isomer with Cl *trans* to the coordinated P=S group. [g] δ(P$_D$Et$_3$) 18.1 ppm, J(P$_A$–P$_D$) nr, J(P$_B$–P$_D$) nr, J(P$_C$–P$_D$) 430, J(Pt–P$_D$) 2457 Hz. [h] Less than 40 Hz (see text). [i] δ(PEt$_3$) 15.3 ppm, J(P$_A$–P$_D$) 43, J(P$_B$–P$_D$) 12, J(P$_C$–P$_D$) 423, J(Pt–P$_D$) 2396 Hz. [j] Acetone solution with an external C$_6$D$_6$ lock. P$_A$ and P$_B$ are averaged by exchange (see text). δ(PEt$_3$) 30.7 ppm, J(P$_{A/B}$–P$_D$) 22, J(P$_C$–P$_D$) 484.

TABLE 2. Crystallographic data for **1**, CH(PPh$_2$)(P(S)Ph$_2$)$_2$, and **3a**, [Ir(cod){CH(PPh$_2$)(P(S)Ph$_2$)$_2$-*P,S,S*}]BF$_4$·CH$_2$Cl$_2$

	1	**3a**
Formula	$C_{37}H_{31}P_3S_2$	$C_{46}H_{45}BCl_2F_4P_3S_2Ir$
fw	632.7	1104.8
Space group	$P2_1/n$ (No 14)	$P\bar{1}$ (No.2)
a, Å	19.867(9)	10.899(6)
b, Å	18.889(7)	21.653(9)
c, Å	8.828(4)	11.124(5)
α, deg	90	85.14(5)
β, deg	100.47(5)	111.59(4)
γ, deg	90	107.93(6)
V, Å^3	3260	2321
Z	4	2
Diffractometer	Picker 4-circle	Picker 4-circle
Radiation (λ, Å)	Mo-Kα (0.71069)	Mo-Kα (0.71069)
μ, cm^{-1}	3.31	34.72
Transm factor range	0.91–0.93	0.47–0.75
Temperature, K	295	295
No. of obs. reflcns. ($I > 3.0\ \sigma(I)$)	2469	4997
Parameters refined	209	356
R	0.059	0.056
R_w	0.073	0.071
GOF	1.59	1.69

$w = 1/(\sigma^2(F)+0.001F^2)$; $\Delta = ||F_o| - |F_c||$. $R = (\Sigma\Delta/\Sigma F_o)$; $R_w = (\Sigma w\Delta^2/\Sigma wF_o^2)^{1/2}$.

^{31}P NMR spectra were recorded in appropriate solvents (Table 1) at 101.3 MHz, using a Bruker WM250 Fourier transform spectrometer. Protons were decoupled by broad-band ("noise") irradiation, and a lock signal was derived from the deuterium resonance of a capilliary insert containing C_6D_6. ^{31}P chemical shifts were measured relative to external P(OMe)$_3$, and are reported in parts per million relative to 85% H_3PO_4 using a conversion factor of +141 ppm. Positive chemical shifts are downfield of the reference.

All operations were carried out at ambient temperature (*ca.* 25°C) under an atmosphere of dry nitrogen using standard Schlenk tube techniques. Solvents were dried by reflux over appropriate reagents (calcium hydride for dichloromethane, and potassium/benzophenone for diethyl ether, toluene, and hexane) and were distilled under nitrogen prior to use. Recrystallizations from solvent pairs were performed by dissolution of the complex in the first solvent (using about double the volume required for complete solution) followed by dropwise addition of sufficient second solvent to cause turbidity at ambient temperature. Crystallization was then completed either by continued very slow dropwise addition of the second solvent or by setting the mixture aside at a reduced temperature.

The ligand CH(PPh$_2$)(P(S)Ph$_2$)$_2$ [15], and the metal complexes, [M$_2$Cl$_2$(cod)$_2$], M = Rh or Ir [16,17], and [M$_2$Cl$_4$(PEt$_3$)$_2$], M = Pd or Pt [18], were prepared as previously described.

2.1.1. [Ir(cod){CH(PPh$_2$)(P(S)Ph$_2$)$_2$-P,S,S}]BF$_4$ · CH$_2$Cl$_2$ 3A

A solution of NaBF$_4$ (0.033 g, 0.30 mmol) in 1:1 ethanol/water (2 mL) was added dropwise to a stirred solution of CH(PPh$_2$)(P(S)Ph$_2$)$_2$ (0.19 g, 0.30 mmol)

TABLE 3. Fractional atomic coordinates and temperature parameters for **1**, CH(PPh$_2$)(P(S)Ph$_2$)$_2$

Atom	x	y	z	U_{eq}
S(1)	1223(1)	4129(1)	3882(2)	53(1)
S(2)	861(1)	1681(1)	7683(2)	55(1)
P(1)	1521(1)	3592(1)	5757(2)	38(1)
P(2)	736(1)	2110(1)	5633(2)	37(1)
P(3)	1845(1)	2393(1)	3610(2)	43(1)
H(1)	190(4)	245(4)	607(9)	7(3)'
C(1)	1525(4)	2617(3)	5450(8)	37(2)
C(11)	2399(3)	3791(4)	6672(8)	42(2)'
C(12)	2763(4)	3389(4)	7864(9)	56(2)'
C(13)	3442(4)	3570(4)	8499(10)	67(2)'
C(14)	3733(4)	4139(4)	7952(9)	66(2)'
C(15)	3392(4)	4544(4)	6794(10)	66(2)'
C(16)	2715(4)	4373(4)	6143(9)	54(2)'
C(21)	1015(3)	3770(4)	7242(8)	44(2)'
C(22)	1139(4)	3439(4)	8652(8)	50(2)'
C(23)	737(4)	3588(4)	9744(10)	64(2)'
C(24)	217(5)	4069(4)	9413(11)	75(3)'
C(25)	99(4)	4413(5)	8034(10)	74(3)'
C(26)	497(4)	4271(4)	6922(9)	56(2)'
C(31)	613(3)	1429(3)	4135(8)	35(2)'
C(32)	686(3)	726(3)	4580(8)	44(2)'
C(33)	622(4)	197(4)	3472(9)	52(2)'
C(34)	502(4)	367(4)	1943(9)	57(2)'
C(35)	429(4)	1056(4)	1473(9)	55(2)'
C(36)	475(3)	1587(4)	2571(8)	46(2)'
C(41)	−16(3)	2679(4)	5193(8)	43(2)'
C(42)	−181(4)	3055(4)	3831(9)	52(2)'
C(43)	−776(4)	3465(5)	3559(11)	75(3)'
C(44)	−1195(5)	3474(5)	4648(11)	84(3)'
C(45)	−1033(5)	3119(4)	5997(11)	77(3)'
C(46)	−439(4)	2711(4)	6278(9)	56(2)'
C(51)	2663(3)	2874(3)	3710(8)	40(2)'
C(52)	3259(4)	2702(4)	4714(9)	50(2)'
C(53)	3872(4)	3039(4)	4565(9)	56(2)'
C(54)	3870(4)	3551(4)	3460(9)	59(2)'
C(55)	3280(4)	3738(4)	2503(9)	54(2)'
C(56)	2673(4)	3389(4)	2621(9)	50(2)'
C(61)	2215(3)	1503(4)	4070(8)	44(2)'
C(62)	2385(4)	1188(4)	5483(10)	60(2)'
C(63)	2738(4)	528(5)	5659(12)	79(3)'
C(64)	2895(5)	219(5)	4393(12)	88(3)'
C(65)	2732(5)	513(5)	2987(13)	92(3)'
C(66)	2371(4)	1162(5)	2774(11)	72(2)'

Estimated standard deviations are given in parentheses. Coordinates $\times 10^n$ where $n = 4$ for S,P,C and 3 for H. Temperature parameters $\times 10^n$ where $n = 3$ for S,P,C, and 2 for H. U_{eq} = the equivalent isotropic temperature parameter $= 1/3\Sigma_i\Sigma_j U_{ij}a_i^*a_j^*(a_i.a_j)$. Primed values indicate that U_{iso} is given, where $T = \exp-(8\pi^2U_{iso}\sin^2\theta/\lambda^2)$.

TABLE 4. Fractional atomic coordinates and temperature parameters for **3a**, $[Ir(cod)\{CH(PPh_2)(P(S)Ph_2)_2\text{-}P,S,S\}]BF_4 \cdot CH_2Cl_2$

Atom	x	y	z	U_{eq}
Ir(1)	68801(4)	30720(2)	15037(4)	349(2)
S(1)	6515(3)	1905(1)	1419(3)	45(1)
S(2)	5113(3)	2841(2)	2561(3)	48(1)
P(1)	4395(3)	1504(1)	461(3)	37(1)
P(2)	3278(3)	2548(1)	946(3)	37(1)
P(3)	5025(3)	2803(1)	−622(2)	34(1)
H(1)	2677(21)	2050(19)	−1118(21)	37(2)′
C(1)	3580(9)	2165(4)	−286(8)	31(1)
C(11)	3701(10)	1021(5)	1552(9)	41(2)′
C(12)	2344(11)	561(6)	1044(10)	57(2)′
C(13)	1860(13)	162(7)	1930(12)	76(2)′
C(14)	2843(12)	198(6)	3303(11)	71(2)′
C(15)	4169(12)	638(6)	3784(10)	62(2)′
C(16)	4651(11)	1062(5)	2937(10)	50(2)′
C(21)	3901(10)	936(5)	−923(9)	41(2)′
C(22)	2498(11)	729(6)	−1901(10)	53(2)′
C(23)	2193(12)	269(6)	−2939(11)	66(2)′
C(24)	3285(12)	53(6)	−2881(11)	69(2)′
C(25)	4626(12)	268(6)	−1970(11)	67(2)′
C(26)	4992(11)	739(5)	−916(10)	51(2)′
C(31)	1863(10)	2005(5)	1269(9)	44(2)′
C(32)	2076(12)	1985(6)	2626(11)	66(2)′
C(33)	843(14)	1589(7)	2888(12)	89(2)′
C(34)	−409(14)	1299(8)	1867(13)	92(2)′
C(35)	−622(13)	1320(7)	519(12)	83(2)′
C(36)	529(12)	1676(6)	212(11)	63(2)′
C(41)	2571(10)	3211(5)	155(9)	43(2)′
C(42)	3119(11)	3798(6)	913(10)	56(2)′
C(43)	2515(11)	4303(6)	377(10)	60(2)′
C(44)	1389(12)	4216(6)	−868(11)	69(2)′
C(45)	823(11)	3626(6)	−1624(10)	61(2)′
C(46)	1390(11)	3104(5)	−1115(10)	50(2)′
C(51)	5397(10)	2406(5)	−1765(9)	38(2)′
C(52)	4328(10)	2013(5)	−2913(9)	45(2)′
C(53)	4738(11)	1797(6)	−3779(10)	61(2)′
C(54)	6157(12)	1934(6)	−3529(11)	68(2)′
C(55)	7208(12)	2299(6)	−2369(11)	67(2)′
C(56)	6831(11)	2550(5)	−1495(10)	52(2)′
C(61)	4102(10)	3350(5)	−1762(9)	40(2)′
C(62)	4587(11)	3996(5)	−1433(10)	50(2)′
C(63)	3972(12)	4444(6)	−2342(11)	67(2)′
C(64)	2877(12)	4193(6)	−3586(11)	65(2)′
C(65)	2360(12)	3550(6)	−3913(11)	67(2)′
C(66)	2956(11)	3103(6)	−2978(10)	56(2)′
C(71)	8597(11)	3180(6)	3509(10)	59(2)
C(72)	9102(11)	3085(6)	2590(11)	58(2)
C(73)	10147(11)	3621(7)	2172(13)	83(2)
C(74)	9495(12)	4073(7)	1263(12)	79(2)
C(75)	7951(10)	3958(5)	929(10)	50(2)
C(76)	7385(11)	4092(5)	1818(9)	46(2)
C(77)	8397(14)	4342(6)	3293(11)	93(2)
C(78)	8936(14)	3846(7)	4190(11)	86(2)
B(1)	547(14)	8461(8)	4028(13)	76(2)
F(1)	−111(12)	8500(6)	2755(9)	164(2)
F(2)	1816(11)	8674(8)	4649(12)	202(2)
F(3)	416(17)	7918(9)	4228(17)	445(2)
F(4)	−15(17)	8697(12)	4405(14)	506(2)
C(80)	4066(15)	6238(8)	4124(13)	106(2)
Cl(1)	4925(8)	5790(3)	5387(5)	153(1)
Cl(2)	2437(7)	5728(4)	2962(7)	174(2)

Notes to Table 4.

Estimated standard deviations are given in parentheses. Coordinates $\times 10^n$ where $n = 5$ for Ir, and 4 otherwise. Temperature parameters $\times 10^n$ where $n = 4$ for Ir, and 3 otherwise. U_{eq} = the equivalent isotropic temperature parameter $= 1/3\Sigma_i\Sigma_j U_{ij} a_i^* a_j^* (a_i . a_j)$. Primed values indicate that U_{iso} is given, where $T = \exp -(8\pi^2 U_{iso} \sin^2\theta / \lambda^2)$.

and $[Ir_2Cl_2(cod)_2]$ (0.10 g, 0.15 mmol) in dichloromethane (10 mL). After 10 min the solvent was removed *in vacuo* and the residue extracted with dichloromethane (10 mL). Solvent was removed from the extract *in vacuo* and the resulting residue washed with hexane (3 × 5 mL) and recrystallized from dichloromethane/hexanes to give $[Ir(cod)\{CH(PPh_2)(P(S)Ph_2)_2\text{-}P,S,S\}]BF_4 \cdot CH_2Cl_2$ as orange crystals (0.25 g, 0.23 mmol). Anal. Found: C, 50.0; H, 4.23. Calc. for $C_{46}H_{45}BCl_2F_4P_3S_2Ir$: C, 50.0; H, 4.11%.

2.1.2. $[Rh(cod)\{CH(PPh_2)(P(S)Ph_2)_2\text{-}P,S,S\}]BF_4$ **3B**

Preparation of this complex was attempted by a procedure similar to that used above for the iridium analog. ^{31}P NMR spectra (Table 1) indicated that the desired product was obtained but it was always contaminated by about 20% of the deprotonated complex, $[Rh(cod)\{C(PPh_2)(P(S)Ph_2)_2\text{-}P,S\}]$. We have described preparation of the deprotonated complex previously [14]. Reaction of the deprotonated complex with acid (CF_3COOH) followed by base ($NHEt_2$) indicated that the complexes are readily interconverted, but we were unable to isolate pure samples of $[Rh(cod)\{CH(PPh_2)(P(S)Ph_2)_2\text{-}P,S,S\}]BF_4$.

2.1.3. $[PdCl(PEt_3)\{CH(PPh_2)(P(S)Ph_2)_2\text{-}P,S\}]BF_4$ **4B**

$CH(PPh_2)(P(S)Ph_2)_2$ (0.12 g, 0.19 mmol) was added to a stirred solution of $[Pd_2Cl_4(PEt_3)_2]$ (0.053 g, 0.09 mmol) with $NaBF_4$ (0.022 g, 0.20 mmol) in acetone (15 mL). After 30 min the solvent was removed *in vacuo* and the residue extracted with dichloromethane (10–15 mL). Solvent was removed from the extract *in vacuo* and the resulting residue recrystallized from dichloromethane/hexanes to give $[PdCl(PEt_3)\{CH(PPh_2)(P(S)Ph_2)_2\text{-}P,S\}]BF_4$ as yellow crystals (0.14 g, 0.14 mmol). Anal. Found: C, 52.5; H, 4.49. Calc. for $C_{43}H_{46}BF_4ClP_4S_2Pd$: C, 52.7; H, 4.73%. ^{31}P NMR spectra showed that the product was mainly isomer **4(i)** with about 15% of **4(ii)**.

2.1.4. $[PtCl(PEt_3)\{CH(PPh_2)(P(S)Ph_2)_2\text{-}P,S\}]BF_4$ **4A**

This complex was prepared by a procedure similar to that used above for the palladium analog. $[PtCl(PEt_3)\{C(PPh_2)(P(S)Ph_2)_2\text{-}P,S\}]BF_4$ was obtained as yellow crystals in 75% yield. Anal. Found: C, 48.1;

TABLE 5. Selected interatomic distance (Å) and bond angles (°) for **1**, $CH(PPh_2)(P(S)Ph_2)_2$

Distances			
S(1)–P(1)	1.941(3)	P(2)–C(1)	1.868(7)
S(2)–P(2)	1.958(3)	P(2)–C(31)	1.830(7)
C(1)–H(1)	0.90(7)	P(2)–C(41)	1.825(7)
P(1)–C(1)	1.863(7)	P(3)–C(1)	1.896(7)
P(1)–C(11)	1.824(7)	P(3)–C(51)	1.850(7)
P(1)–C(21)	1.823(7)	P(3)–C(61)	1.850(7)
Angles			
S(1)–P(1)–C(1)	113.7(3)	C(31)–P(2)–C(41)	105.3(3)
S(1)–P(1)–C(11)	112.8(2)	C(1)–P(3)–C(51)	106.1(3)
S(1)–P(1)–C(21)	113.2(2)	C(1)–P(3)–C(61)	101.4(3)
C(1)–P(1)–C(11)	103.8(3)	C(51)–P(3)–C(61)	97.2(3)
C(1)–P(1)–C(21)	107.8(3)	P(1)–C(1)–H(1)	106(5)
C(11)–P(1)–C(21)	104.6(3)	P(2)–C(1)–H(1)	113(5)
S(2)–P(2)–C(1)	109.0(2)	P(3)–C(1)–H(1)	94.0(5)
S(2)–P(2)–C(31)	110.8(2)	P(1)–C(1)–P(2)	117.9(4)
S(2)–P(2)–C(41)	113.7(2)	P(1)–C(1)–P(3)	110.9(3)
C(1)–P(2)–C(31)	107.6(3)	P(2)–C(1)–P(3)	112.1(3)
C(1)–P(2)–C(41)	110.3(3)		

Estimated standard deviations are given in parentheses.

TABLE 6. Selected interatomic distances (Å) and bond angles (°) for **3a**, $[Ir(cod)\{CH(PPh_2)(P(S)Ph_2)_2\text{-}P,S,S\}]BF_4 \cdot CH_2Cl_2$

Distances			
Ir(1)–S(1)	2.438(3)	P(1)–C(1)	1.863(9)
Ir(1)–S(2)	2.574(3)	P(1)–C(11)	1.798(10)
Ir(1)–P(3)	2.314(2)	P(1)–C(21)	1.834(10)
Ir(1)–C(71)	2.170(9)	P(2)–C(1)	1.852(9)
Ir(1)–C(72)	2.177(10)	P(2)–C(31)	1.784(10)
Ir(1)–C(75)	2.125(11)	P(2)–C(41)	1.817(10)
Ir(1)–C(76)	2.125(10)	P(3)–C(1)	1.900(9)
S(1)–P(1)	2.001(4)	P(3)–C(51)	1.834(10)
S(2)–P(2)	1.977(4)	P(3)–C(61)	1.842(9)
H(1)–C(1)	0.99(2)		
Angles			
S(1)–Ir(1)–S(2)	87.8(1)	S(2)–P(2)–C(1)	108.2(3)
S(1)–Ir(1)–P(3)	81.1(1)	S(2)–P(2)–C(31)	113.8(3)
S(1)–Ir(1)–C*x*	86.8	S(2)–P(2)–C(41)	113.0(3)
S(1)–Ir(1)–C*y*	161.2	C(1)–P(2)–C(31)	110.6(4)
S(2)–Ir(1)–P(3)	91.5(1)	C(1)–P(2)–C(41)	107.6(4)
S(2)–Ir(1)–C*x*	106.4	C(31)–P(2)–C(41)	103.5(5)
S(2)–Ir(1)–C*y*	110.6	Ir(1)–P(3)–C(1)	102.2(3)
P(3)–Ir(1)–C*x*	159.1	Ir(1)–P(3)–C(51)	114.4(3)
P(3)–Ir(1)–C*y*	100.9	Ir(1)–P(3)–C(61)	127.0(3)
C*x*–Ir(1)–C*y*	85.5	C(1)–P(3)–C(51)	106.5(4)
Ir(1)–S(1)–P(1)	105.0(1)	C(1)–P(3)–C(61)	104.9(4)
Ir(1)–S(2)–P(2)	100.2(1)	C(51)–P(3)–C(61)	100.1(4)
S(1)–P(1)–C(1)	108.1(3)	P(1)–C(1)–H(1)	117(3)
S(1)–P(1)–C(11)	111.1(3)	P(2)–C(1)–H(1)	108(2)
S(1)–P(1)–C(21)	111.7(3)	P(3)–C(1)–H(1)	110(2)
C(1)–P(1)–C(11)	114.1(4)	P(1)–C(1)–P(2)	111.0(4)
C(1)–P(1)–C(21)	107.0(4)	P(1)–C(1)–P(3)	104.0(4)
C(11)–P(1)–C(21)	104.9(5)	P(2)–C(1)–P(3)	106.7(4)

Estimated standard deviations are given in parentheses. C*x* is the mid-point of the C(71)–C(72) bond and C*y* is the mid-point of the C(75)–C(76) bond.

H, 4.24. Calc. for $C_{43}H_{46}BF_4ClP_4S_2Pt$: C, 48.4; H, 4.34%. ^{31}P NMR spectra showed that the product was almost entirely isomer **4(i)** with only traces of **4(ii)**.

2.2. X-ray data collection

Compounds **1**, $CH(PPh_2)(P(S)Ph_2)_2$ and **3a**, $[Ir(cod)\{CH(PPh_2)(P(S)Ph_2)_2\text{-}P,S,S\}]BF_4 \cdot CH_2Cl_2$, were prepared as described above, and crystals suitable for study by X-ray diffraction were grown by vapour diffusion of hexane (**1**) or diethyl ether (**3a**) into solutions of the complexes in dichloromethane.

Preliminary photographic work was carried out with Weissenberg and precession cameras using Cu–Kα radiation. After establishment of symmetry and approximate unit cells the crystals were transferred to a Picker 4-circle diffractometer automated with a PDP11/10 computer, and the unit cells refined by least-squares methods employing pairs of centering measurements (Table 2). During the subsequent data collection there was no evidence of decomposition of either crystal. Data collection used a $\theta/2\theta$ step scan with 200 steps of 0.01° in 2θ for **1**, and 160 steps for **3a**, with counting for 0.25 s per step. Background measurements were for 25 s at each end of the scan for **1**, 20 s for **3a**. Each batch of 50 reflections was preceded by the measurement of three standard reflections, and, after application of Lorentz and polarization factors, each batch was scaled to maintain the sum of the standards constant. Absorption corrections were applied by a numerical integration using a Gaussian grid and with the crystal shape defined by perpendicular distances to crystal faces from a central origin.

2.3. Structure solution and refinement

The structures were found and refined using the SHELX-76 program package [19] and illustrations were drawn using ORTEP [20]. The atomic scattering factors used were for neutral atoms, with corrections for anomalous dispersion [21]. The structures were solved by direct methods, developed by standard Fourier synthesis procedures using difference maps, and refined by the method of least squares minimising $\Sigma w\Delta^2$ where $\Delta = \left| |F_o| - |F_c| \right|$. The weights were obtained from counting statistics using $w = 1/(\sigma^2(F) + 0.001F^2)$. The iridium atom, and all phosphorus, sulfur, chlorine, boron and fluorine atoms were treated anisotropically, as were the central ligand carbons, C(1) in both structures, the carbon of the dichloromethane, and the carbons of the cod ligand, C(71–78) in **3a**. All other atoms were treated isotropically. The methine hydrogens, H(1), were located in both structures. Other hydrogen atoms were not located and are not included in the refinement for structure **3a**. For structure **1**, the phenyl ring hydrogen positions were calculated and allowed to ride on their respective carbon atoms during the refinement. Each ring was treated separately but, within each ring, the hydrogens were refined using a common temperature factor. For structure **3a**, we carried out a trial refinement with variable site occupancy factors for the CH_2Cl_2 molecule, but there was no significant departure from full occupancy. The final difference maps had significant residuals only close to the heavy atoms in **1**, or to the iridium or the BF_4 group in **3a**, and gave no indication that any material had been overlooked.

3. Results and discussion

3.1. Synthesis

The ligand, $CH(PPh_2(P(S)Ph)_2)_2]$ **1**, reacts smoothly under mild conditions with the chlorobridged complexes, $[M_2Cl_2(cod)_2]$, M = Rh or Ir, cod = cycloocta-1,5-diene, and $[M_2Cl_4(PEt_3)_2]$, M = Pt or Pd. The products are complex cations, $[M(cod)\{CH(PPh_2)(P(S)Ph_2)_2\text{-}P,S,S\}]^+$ **3**, and $[MCl(PEt_3)\{CH(PPh_2)(P(S)Ph_2)_2\text{-}P,S,S\}]^+$ **4**, and addition of $NaBF_4$ to the reactions enables their isolation as fluoroborate salts. When M = Rh, the reaction is always accompanied by partial deprotonation of the ligand to contaminate the product with $[Rh(cod)\{C(PPh_2)(P(S)Ph_2)_2\text{-}P,S,S\}]$. As we have reported previously, reactions in the presence of base ($NHEt_2$) result in deprotonated products for all the metals [14].

3.2. ^{31}P Nuclear magnetic resonance

$^{31}P\{^1H\}$ NMR parameters for the complexes are collected in Table 1, and the atom labelling schemes are shown in Scheme 1. The previously reported spectrum of $[Ir(cod)\{C(PPh_2)(P(S)Ph_2)_2\text{-}P,S\}]$, showed three resonances as expected for η^2-*P,S* coordination (Scheme 1, structure **2a**). In contrast, the spectrum of the protonated complex, $[Ir(cod)\{CH(PPh_2)(P(S)Ph_2)_2\text{-}P,S,S\}]^+$ **3a**, consists of only two resonances; a triplet at 37.3 ppm and a doublet at 52.8 ppm with a mutual coupling of 39 Hz. The triplet shift is similar to that assigned to the directly coordinated phosphorus (P_c) of **2a** but the doublet shift is intermediate between the coordinated (65.6 ppm) and non-coordinated (41.7 ppm) P=S groups of **2a**.. A similar situation pertains with the couplings because $^2J(P-P)$ in **3a** is intermediate between the P_A-P_C and P_B-P_C values of **2a**. This comparison raises the possibility that **3a** has a structure analogous to **2a** but with dynamic exchange between the two P=S groups. However, spectra recorded down to −90°C gave no indication of any slowing of such a dynamic process, and prompted us to examine the complex by X-ray diffraction (below) which confirmed that the complex does indeed contain a tripodal η^3-*P,S,S* ligand as in structure **3a**. This does not, of course, exclude the possibility of some dynamic process in solution, and indeed some motion is probably required to produce exact equivalence of the P_A and P_B resonances. Spectra of the rhodium analog, $[Rh(cod)\{CH(PPh_2)(P(S)Ph_2)_2\text{-}P,S,S\}]^+$ **3b**, are similar except, of course, for the addition of Rh–P coupling.

In contrast, $[PtCl(PEt_3)\{CH(PPh_2)(P(S)Ph_2)_2\text{-}P,S\}]^+$ **4a**, shows a spectrum much more closely analogous to that of its deprotonated relative, $[PtCl(PEt_3)\{C(PPh_2)(P(S)Ph_2)_2\text{-}P,S\}]$, with three separate ^{31}P resonances indicative of an η^2-*P,S* structure. The large coupling (430 Hz) of P_c to the phosphorus of the PEt_3 ligand shows a *trans* geometry (isomer **4a(i)**), a conclusion which is supported by the relatively small $^1J(Pt-P)$ values (2350 Hz and 2457 Hz). The spectrum also showed the presence of traces of the other isomer, **4a(ii)**, but not in sufficient quantities for a reliable assignment. Interestingly, this isomer distribution is the reverse of that observed previously for the deprotonated complex, $[PtCl(PEt_3)\{C(PPh_2)(P(S)Ph_2)_2\text{-}P,S\}]$, where about 90% of the product consisted of the isomer analogous to **4a(ii)**. A further interesting point concerns the relative magnitudes of the 2-bond and 3-bond Pt–P coupling constants. In deprotonated complexes [14], there was some ambiguity regarding the assignment of P_A and P_B, with the weight of evidence favouring the assignment shown in Table 1. This assignment is slightly unusual in that $^3J(M-P) > {}^2J(M-P)$, respectively 197 Hz and 78 Hz in $[PtCl(PEt_3)\{C(PPh_2)(P(S)Ph_2)_2\text{-}P,S\}]$. In marked contrast, the two-bond coupling in **4a(i)** is 117 Hz, while the 3-bond coupling is not resolved in the observed spectrum. Line width considerations suggest that it cannot be larger than about 40 Hz. Thus, in the M–P–C–P chain, the hybridization of the carbon has a dramatic effect on the 3-bond coupling, with small values for an sp^3 carbon (< 40 Hz) and much larger values (197 Hz) for an sp^2 carbon. Similar effects pertain in rhodium complexes, although the much smaller metal-phosphorus coupling make the observations more problematical.

Moving finally to the palladium complex, $[PdCl(PEt_3)\{CH(PPh_2)(P(S)Ph_2)_2\text{-}P,S\}]^+$ **4b**, we again find a spectrum with only two phosphorus resonances for the phosphine chalcogenide ligand. The parameters, $\delta(P_A/P_B)$, $J(P_A/P_B-P_C)$, and $J(P_A/P_B-P_D)$, are all close to the averages of corresponding parameters in the platinum analog. It is most likely, therefore, that the structure is **4b(i)** and that the generally more labile coordination sphere of palladium results in dynamic exchange between the coordinated and non-coordinate P=S groups. We were not successful in freezing this exchange by low temperature spectroscopy. The spectra also show the presence of about 15–20% of isomer

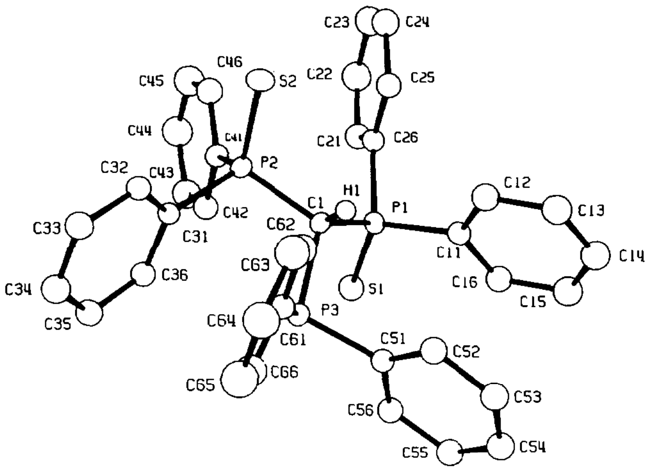

Fig. 1. ORTEP plot for a single molecule of **1**, CH(PPh$_2$(P(S)Ph$_2$)$_2$.

4b(ii), but, as for the platinum analog, overlapping of resonances and low intensities preclude a reliable assignment.

3.3. X-ray crystal structures

The atom labelling schemes and structures of single molecules of the ligand **1**, CH(PPh$_2$)(P(S)Ph$_2$)$_2$, and complex **3a**, [Ir(cod){CH(PPh$_2$)(P(S)Ph$_2$)$_2$-*P,S,S*}]BF$_4$ · CH$_2$Cl$_2$, are shown as ORTEP diagrams in Figs. 1 and 2 respectively. Unit cell and other parameters related to the crystal structure determinations are in Table 2. Fractional atomic coordinates and isotropic temperature parameters are given in Tables 3 and 4, and the most significant bond lengths and angles are collected in Tables 5 and 6 [22*].

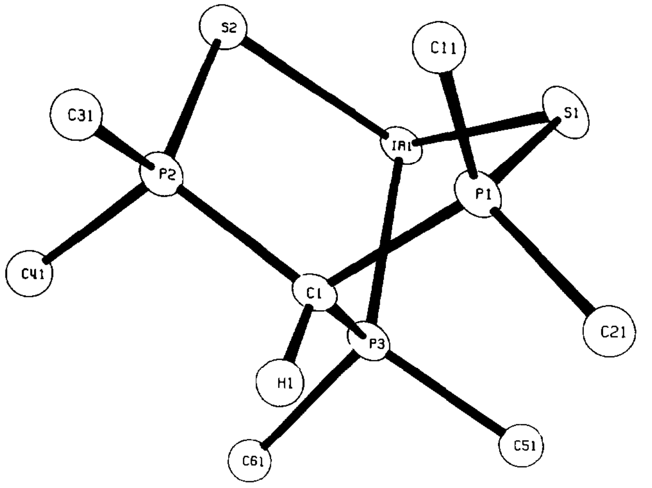

Fig. 2. ORTEP plot for a single cation of **3a**, [Ir(cod){CH(PPh$_2$)(P(S)Ph$_2$)$_2$-*P,S,S*}]BF$_4$·CH$_2$Cl$_2$. In the interests of clarity, each phenyl ring is represented only by the carbon directly bound to phosphorus, and the cod ligand has been omitted.

Comparison of the ligand, **1**, with its trisulfide relative, CH(P(S)Ph$_2$)$_3$ shows no significant differences in parameters. The P=S lengths are similar, averaging 1.95 Å and 1.94 Å respectively, and similar comparisons hold for other lengths and angles except for some small changes associated with the P(III) group. For example, the C–PPh$_2$ bond (1.898(7) Å) in **1** is slightly longer than the C–P(S)Ph$_2$ bonds (1.865(7) Å).

Coordination of the ligand to iridium produces relatively little change in the ligand except for the geometry of C(1) which is discussed below. The complex cation, **3a**, contains a tripodal η^3-*P,S,S* coordinated ligand, with S–Ir–S and S–Ir–P angles ranging from 81° to 92°. An irregular five-coordinate geometry about the iridium is completed by the two double bonds of the cod ligand. The Ir–S bonds average 2.50 Å, significantly longer than those found in the bidentate, η^2-*S,S* complex, [Ir(CO)$_2${CH(P(S)Ph$_2$)$_3$-*S,S*}], average 2.36 Å [8]. In both complexes, comparison with free ligand parameters indicates a small but consistent lengthening of the P–S bonds on coordination. Thus, considering average P–S lengths, between **1** and **3a**, the change is from an average of 1.95 Å to 1.99 Å, and between CH(P(S)Ph$_2$)$_3$ and [Ir(CO)$_2${CH(P(S)Ph$_2$)$_3$-*S,S*}], 1.94 Å to 2.06 Å, consistent with the view that Ir–S bonding is weaker in **3a** than in the bidentate complex.

The most interesting structural consideration involves the geometry at the central carbon, C(1), of the phosphine chalcogenide ligand. In the free ligand, **1**, this carbon lies 0.48 Å out of the plane defined by P(1–3), and the P–C–P angles average 114°, consistent with an sp^3 geometry which has been slightly distorted by the bulky attachments. In the deprotonated tripodal structures reported by Grim and co-workers, [HgCl{C(P(S)Me$_2$)(P(S)Ph$_2$)$_2$-*S,S,S*}] [3] and [Ag(PBu$_3$){C(P(S)Ph$_2$)$_3$-*S,S,S*}] [5], the corresponding displacements are 0.34 Å and 0.36 Å, and the angles average 116° in both cases, consistent with a flattening of the CP$_3$ unit when the carbon approaches sp^2 hybridization. In complex **3a**, the displacement of C(1) from the P(1–3) plane is 0.73 Å and the P–C–P angles average 107°. This is important confirmation that the carbon is indeed protonated, and it also shows the narrowing of the P–C–P angles needed to achieve tripodal coordination. With respect to whether tripodal coordination is easier in the protonated or deprotonated ligands, we note that distortion is needed in both cases. However, one would expect that narrowing of the angles in a basically sp^3 geometry would be easier than the marked distortion of the planar sp^2 geometry which is necessary in the deprotonated ligands.

---

* Reference number with asterisk refers to a note in the list of references.

Acknowledgments

We thank the Natural Sciences and Engineering Research Council of Canada and the University of Victoria for research grants, Mrs. K. Beveridge for technical assistance in the crystal structure determinations, and Mrs C. Greenwood for recording NMR spectra.

References and notes

1 S.O. Grim and S.A. Sangokoya, *J. Chem. Soc., Chem. Commun.*, (1984) 1599.

2 S.O. Grim, S.A. Sangokoya, R.D. Gilardi, I.J. Colquhoun and W. McFarlane, *23rd Int. Conf. on Coordination Chemistry, Boulder, Colorado*, 1984.

3 S.O. Grim, P.H. Smith, S. Nittolo, H.L. Ammon, L.C. Satek, S.A. Sangokoya, R.K. Khanna, I.J. Colquhoun, W. McFarlane and J.R. Holden, *Inorg. Chem.*, **24** (1985) 2889.

4 S.O. Grim, S.A. Sangokoya, I.J. Colquhoun, W. McFarlane and R.K. Khanna, *Inorg. Chem.*, **25** (1986) 2699.

5 S.O. Grim, S.A. Sangokoya, A.L. Rheingold, W. McFarlane, I.J. Colquhoun and R.D. Gilardi, *Inorg. Chem.*, *30* (1991) 2519.

6 S.O. Grim, P.B. Kettler and J.B. Thoden, *Organometallics*, *10* (1991) 2399.

7 J. Browning, K.A. Beveridge, G.W. Bushnell and K.R. Dixon, *Inorg. Chem.*, *25* (1986) 1987.

8 J. Browning, K.R. Dixon, R.W. Hilts, N.J. Meanwell and F. Wang, *J. Organomet. Chem.*, **410** (1991) 389.

9 S. Trofimenko, *Acc. Chem. Res.*, *4* (1971) 17.

10 S. Trofimenko, *Chem. Rev.*, *72* (1972) 497.

11 C.K. Ghosh, D.P.S. Rodgers and W.A.G. Graham, *J. Chem. Soc., Chem. Commun.*, (1988) 1511.

12 R.S. Tanke and R.H. Crabtree, *J. Chem. Soc., Chem. Commun.*, (1990) 1056.

13 R.S. Tanke and R.H. Crabtree, *J. Am. Chem. Soc.*, *112* (1990) 7984.

14 J. Browning, K.R. Dixon, N.J. Meanwell and F. Wang, *J. Organomet. Chem.*, *460* (1993) 117.

15 S.O. Grim, L.C. Satek and J.D. Mitchell, *Z. Naturforsch. B. Anorg. Chem. Org. Chem.*, *35* (1980) 832.

16 J.L. Herde, J.C. Lambert and C.V. Senoff, *Inorg. Synth.*, *15* (1974) 18.

17 G. Giordano and R.H. Crabtree, *Inorg. Synth.*, *19* (1979) 218.

18 R.J. Goodfellow and L.M. Venanzi, *J. Chem. Soc.*, (1965) 7533.

19 G.M. Sheldrick, *SHELX-76*, *A Computer Program for Crystal Structure Determination*, University of Cambridge, Cambridge, UK, 1976.

20 C.K. Johnson, *ORTEP Report ORNL-3794*, Oak Ridge National Laboratory, Oak Ridge, TN, USA, 1965.

21 D.T. Cromer and J.T. Waber in J.A. Ibers and W.C. Hamilton (eds.), *International Tables for X-ray Crystallography*, Vol. IV., Kynoch Press, Birmingham, UK, 1974.

22 Supplementary material, deposited with the Cambridge Crystallographic Dat Cen for compounds **1** and **3a**: unit cell, data collection and refinement parameters (Table S1), fractional atomic coordinates and isotropic temperature parameters for all atoms (Tables S2, S10), anisotropic temperature factors for the heavy atoms (Tables S3, S11), interatomic distances (Tables S4, S12), bond angles (Tables S5, S13), selected intermolecular distances (Tables S6, S14) (15 pages); observed and calculated structure factor amplitudes (Tables S16, S17) (32 pages). For compound **1**: hydrogen atom fractional atomic coordinates isotropic temperature parameters, interatomic distances and bond angles (Tables S7–S9, 3 pages).